Am J Transl Res 2026;18(8):7463-7475
www.ajtr.org /ISSN:1943-8141/AJTR0174070

Original Article

AGTR1 inhibits pyroptosis and inflammatory cytokine secretion in rheumatoid arthritis fibroblast-like synoviocytes through the TGF-β pathway

Jian Wang[1,2], Zongbiao Bai[1,2]

[1]Department of Orthopaedics, Central Hospital of Karamay, Karamay 834000, Xinjiang, China; [2]Department of Orthopaedics, Karamay Hospital of People's Hospital of Xinjiang Uygur Autonomous Region, Karamay 834000, Xinjiang, China

Received May 15, 2026; Accepted August 11, 2026; Epub August 15, 2026; Published August 30, 2026

Abstract: Background: Rheumatoid arthritis (RA) is a chronic, progressive autoimmune disease. The hyperactivation of fibroblast-like synoviocytes (FLS) is a major contributor to synovial hyperplasia and cartilage destruction, and FLS pyroptosis plays a pivotal role in RA pathogenesis. This study aimed to investigate the mechanisms by which AGTR1 regulates FLS pyroptosis and inflammatory cytokine secretion in RA to identify potential therapeutic targets for RA. Methods: Bioinformatic analysis assessed AGTR1 expression levels using the GSE21959 and GSE55235 datasets. qRT-PCR and western blot (WB) measured AGTR1 mRNA and protein levels in cell lines. Nigericin (a pyroptosis inducer), the TGF-β receptor I inhibitor SB505124, and the TGF-β neutralizing antibody 1D11 were administered to AGTR1-overexpressing RA-FLS, followed by western blot analysis of pyroptosis-related proteins. Flow cytometry, LDH assays, and propidium iodide staining evaluated pyroptosis levels. ELISA measured inflammatory cytokine secretion. WB confirmed TGF-β pathway activation. Results: AGTR1 was downregulated in RA-FLS. AGTR1 overexpression suppressed ASC, NLRP3, cleaved caspase-1, and GSDMD-N expression, thereby alleviating pyroptosis in RA-FLS ($P < 0.05$). AGTR1 overexpression inhibited secretion of inflammatory cytokines and reduced lactate dehydrogenase release ($P < 0.05$). We demonstrated that AGTR1-mediated repression of pyroptosis and inflammatory cytokine secretion in RA-FLS was dependent on the TGF-β signaling pathway. Conclusion: AGTR1 inhibits pyroptosis and attenuates inflammatory cytokine secretion in RA-FLS through TGF-β. These findings suggest that AGTR1 induction or TGF-β pathway activation may ameliorate RA pathology.

Keywords: AGTR1, fibroblast-like synoviocytes, pyroptosis, rheumatoid arthritis, TGF-β

Introduction

Rheumatoid arthritis (RA) is a chronic autoimmune disease driven by genetic and environmental factors, characterized by persistent hyperplasia, synovial inflammation, and joint cartilage erosion [1, 2]. Despite the development of biologics and small-molecule inhibitors for RA treatment, a significant proportion of patients remain unresponsive to these therapies [3]. Fibroblast-like synoviocytes (FLS), highly specialized mesenchymal cells in the synovium, are critical for RA pathogenesis [4]. Under physiologic conditions, FLS maintain joint integrity by secretion of synovial fluid and ECM [5]. However, FLS undergo aberrant activation, exhibiting hyperproliferation, invasiveness, and tumor-like transformation. They also secrete proinflammatory cytokines and MMPs, which exacerbate inflammation and joint destruction in RA [6]. Thus, investigating FLS may elucidate the intrinsic mechanisms underlying RA development.

Inflammasome activation and robust proinflammatory mediator release are hallmarks of pyroptosis [7]. The NLRP3 inflammasome recruits and activates caspase-1 through the adaptor protein ASC. Activated caspase-1 cleaves GSDMD into GSDMD-N, which forms membrane pores and induces the release of cytoplasmic contents [7]. Caspase-1 also processes pro-IL-18 and pro-IL-1β into their active forms, which are released extracellularly and amplify inflam-

https://doi.org/10.62347/HTCE3264

mation [8]. FLS pyroptosis contributes significantly to RA pathogenesis [9]. LPS induces pyroptosis in FLS (RSC-364 cells) via the NF-κB-mediated NLRP3/caspase-1/GSDMD and caspase-3/GSDME dual pathways, thereby aggravating RA [10]. Neutrophil extracellular traps promote FLS pyroptosis and phenotypic changes through the NF-κB/caspase-3/GSDME axis [11]. Therefore, elucidating factors modulating FLS pyroptosis may deepen our understanding of RA mechanisms and inform novel therapeutic strategies.

A study on osteoarthritis (OA) revealed that TGF-β1 inhibits chondrocyte pyroptosis through the activation of Smad2/3 and blocking NF-κB, thereby protecting cartilage [12]. TGF-β pathway is a critical regulator of inflammatory responses, essential for maintaining homeostasis, and its dysregulation contributes to immune and inflammatory disorders [13]. In RA, the role of TGF-β signaling has garnered increasing attention [14]. Aberrant TGF-β signaling may exacerbate tissue damage in inflammatory diseases by promoting inflammation and pathologic tissue remodeling [15]. AGTR1, a G protein-coupled receptor, regulates vascular tone, smooth muscle proliferation, extracellular matrix (ECM) production, and inflammation [16]. AGTR1 induces TGF-β expression and enhances TGF-β pathway activity [17], suggesting its involvement in RA progression. However, whether AGTR1 modulates FLS pyroptosis through TGF-β remains unclear and warrants further investigation.

In this study, we explored the regulatory role of AGTR1 in RA-FLS. We demonstrated that AGTR1 was downregulated in RA-FLS, and its overexpression activated the TGF-β pathway, reduced proinflammatory cytokine secretion, and mitigated pyroptosis. These findings highlighted the effect of AGTR1 on FLS pyroptosis and its potential as a target in RA.

Materials and methods

Bioinformatics analysis

Publicly available mRNA expression datasets, GSE21959 and GSE55235, were downloaded from the Gene Expression Omnibus (GEO) database (https://www.ncbi.nlm.nih.gov/geo/) for bioinformatics analysis. Differential expression analysis was performed using the "edgeR" package, with significance thresholds set at |logFC| > 1.5 and padj < 0.05, to identify significantly differentially expressed mRNAs. The GSE21959 dataset is based on the GPL4133 platform (Agilent-014850 Whole Human Genome Microarray 4×44K G4112F) and contains a total of 36 samples derived from *in vitro*-cultured rheumatoid arthritis synovial fibroblasts (RA-SF) and healthy synovial fibroblasts (HSF), encompassing two culture conditions, normoxia and hypoxia (nine RA-SF and nine HSF samples under each condition). To exclude the confounding effect of hypoxic intervention on gene expression, nine RA-SF and nine HSF samples cultured under normoxic conditions were selected for differential analysis. To further validate the expression change of AGTR1 in an independent dataset, an additional dataset, GSE55235, was also incorporated. GSE55235 is based on the GPL96 platform (Affymetrix HG-U133A) and contains a total of 30 samples obtained from synovial tissue biopsy specimens collected during joint replacement surgery or arthroscopy, comprising 10 patients with RA, 10 patients with OA, and 10 healthy controls; this study compared AGTR1 expression between the RA group (n = 10) and the healthy control group (n = 10). The target gene AGTR1 was identified through literature citation, and the differential expression of AGTR1 between healthy controls and RA patients was finally analyzed.

Cell culture and cell line construction

Normal human synovial fibroblasts (NC-FLS, JSY-CC2823) were purchased from Jinshaoyuan (China). RA synovial fibroblasts (RA-FLS, MH7A cell line, CBP61649) were obtained from Cobioer (China). Primary rheumatoid arthritis fibroblast-like synoviocytes (Primary RA-FLS, CP-H248) were purchased from Procell (China). Cells were maintained in RPMI-1640 (Gibco, USA) with 10% FBS at 37°C with 5% CO_2 in a humidified incubator (Thermo Fisher, USA).

pcDNA3.1 empty vector (oe-NC) and pcDNA3.1-*AGTR1* overexpression plasmid (oe-*AGTR1*) were purchased from VectorBuilder (China). MH7A cells and human primary RA-FLS were cultured to 60-70% confluence before transfection. oe-NC and oe-*AGTR1* plasmids were transiently transfected into MH7A cells utilizing Lipofectamine 3000 (Thermo Fisher, USA).

Table 1. Primer sequence

Gene	Sequence (5'-3')
GAPDH	Forward: GGAGCGAGATCCCTCCAAAAT
	Reverse: GGCTGTTGTCATACTTCTCATGG
AGTR1	Forward: GGCTATTGTTCACCCAATGAAGT
	Reverse: TGGGACTCATAATGGAAAGCAC

Transfection efficiency was evaluated at 48 h post-transfection.

RNA extraction and qRT-PCR

Total RNA from MH7A cells was extracted using TRIzol Plus reagent (Takara, Japan), and RNA concentration was measured. cDNA was synthesized with GoScript™ Reverse Transcription Kit (Promega, USA). The resulting cDNA was combined with Fast SYBR™ Green Master Mix (Thermo Fisher Scientific, USA) and subjected to quantitative PCR on an ABI7500 PCR system (Thermo Fisher, USA). Each sample was analyzed in at least three independent experiments. *GAPDH* served as an internal control. Relative mRNA expression was computed using $2^{-\Delta\Delta CT}$. Primer sequences are shown in **Table 1**.

Western blot (WB) analysis

Cells were rinsed with ice-cold PBS and then lysed in RIPA buffer (Beyotime, China) supplemented with 1% PMSF protease inhibitor (Thermo Fisher, USA). Lysates were centrifuged at 14,000×g (4°C, 5 min), and supernatants were harvested. Protein concentration was measured using a BCA kit (Beyotime, China). After separation by SDS-PAGE, proteins were transferred to PVDF. Membranes were sealed with 1% BSA for 2 h, followed by incubation at 4°C with primary antibodies (Abcam) overnight: anti-AGTR1 (ab124734), anti-ASC (ab151700), anti-NLRP3 (ab263899), anti-caspase-1 (ab207802), anti-GSDMD (ab209845), anti-SMAD2 (ab40855), anti-p-SMAD2 (ab280888), anti-TGF-β (ab215715), and anti-GAPDH (ab9485). After rinsing three times with TBST, membranes were incubated with HRP-conjugated goat anti-rabbit IgG (Abcam, ab205718) for 2 h (room temperature). Protein bands were visualized using an ultrasensitive ECL chemiluminescence kit (Beyotime, China) and imaged with Amersham Imager 800 (GE, USA). Band intensity was quantified using the ImageJ software.

TUNEL staining

FLS cells were cultured on coverslips until reaching 60-80% confluency, then fixed with 4% paraformaldehyde in the dark for 15-20 min. After PBS rinses, cells were permeabilized in PBS with 0.1% Triton X-100 for 15 min. Following 3 PBS rinses, 20 μL of TUNEL reaction mixture (Beyotime, China) was added. Cells were incubated at 37°C for 1 h in the dark. The TUNEL reaction mixture was removed, and cells were rinsed with PBS. 5 μL of DAPI-containing antifade mounting medium was added onto the cells. Apoptotic cells were visualized and pictured using a confocal microscope (Olympus, Japan).

Flow cytometry for caspase-1 detection

Caspase-1 and AGTR1 expressions were assessed using FITC-conjugated anti-caspase-1 and anti-AGTR1 antibody kits (Abbexa, UK). RA-FLS cells were trypsinized, centrifuged at 300×g for 5 min, and rinsed with PBS (3 times). Cells were stained with caspase-1 antibody for 15-20 min and analyzed by flow cytometry (BD Calibur, USA).

ELISA for inflammatory cytokine measurement

Secretion of IL-8 (E-EL-H6008), IL-18 (E-EL-H0253), IL-1β (E-EL-H0149), and IL-6 (E-EL-H6156) in RA-FLS supernatants was quantified using ELISA kits (Elabscience, China). Cell supernatants were collected by centrifugation at 300×g for 5 min, and 100 μL of supernatant was added to each well and incubated for 2 h. Liquid was discarded, and 100 μL biotinylated detection antibodies were added for 1 h, followed by HRP-streptavidin conjugate for 20 min in the dark. TMB substrate was added for color development. Distinct coloration developed after approximately 20 min of incubation, and the reaction was subsequently terminated. Absorbance (450 nm) was read by a microplate reader (Thermo Fisher, USA). Cytokine concentrations were computed following standard curves.

LDH release assay

LDH release was assayed with the LDH cytotoxicity kit (Beyotime, China). Cell supernatants (120 μL) were mixed with 60 μL LDH detection reagent and cultured for 30 min away from light

at room temperature. Absorbance (490 nm) was read by microplate reader (Thermo Fisher, USA).

Hoechst 33342/PI staining

Hoechst 33342/propidium iodide (PI) double staining kits (Solarbio, China) were used to detect pyroptosis in RA-FLS of each group. Cells were seeded in 6-well plates at a density of 2×10^5 cells per well and cultured at 37°C with 5% CO_2 for 24 h to allow full adherence, followed by corresponding treatments according to experimental groups. After treatment, the culture medium was aspirated, and cells were gently washed twice with PBS. Subsequently, Hoechst 33342 (5 μg/mL) and PI (2 μg/mL) were sequentially added according to the manufacturer's instructions, and cells were incubated at 37°C in the dark for 15 min. After incubation, cells were washed twice with PBS to remove excessive dye, an appropriate volume of PBS was supplemented, and cells were immediately observed and imaged under a fluorescence microscope. Hoechst 33342 penetrates intact cell membranes and labels all cell nuclei with blue fluorescence, whereas PI only enters cells with compromised membrane integrity and binds to nucleic acids to emit red fluorescence. Accordingly, PI-positive cells (red fluorescence) represent pyroptotic cells. ImageJ software was utilized to calculate quantitatively the proportion of PI-positive cells relative to the total cell count in each field of view, with no fewer than three random fields selected for statistical analysis per group.

It should be noted that LDH release and PI positivity reflect plasma membrane integrity disruption, which is not specific to pyroptosis; therefore, these were used as supplementary indicators alongside the specific pyroptosis markers (GSDMD-N, cleaved caspase-1, etc.) detected by western blot and flow cytometry.

Statistical analysis

All experiments were performed in triplicate, and quantitative data were presented as mean ± standard deviation (SD). Statistical analyses were performed using GraphPad Prism 8.0 software (GraphPad Software, USA). The independent two-sample t-test was adopted for comparisons between two groups, while one-way analysis of variance (ANOVA) followed by Tukey's post-hoc test was applied for comparisons among three or more groups. All statistical tests were two-tailed. Exact *p*-values were labeled directly on figures, and differences with $P < 0.05$ were considered significant.

Results

Downregulation of AGTR1 in RA

We first performed bioinformatic analysis of AGTR1 expression in the GSE21959 dataset, which contains *in vitro*-cultured RA-SF (n = 9) and HSF (n = 9). As shown in the left panel of **Figure 1A**, AGTR1 expression in RA-SF was significantly lower than that in HSF. To further validate this finding, we analyzed the GSE55235 dataset, which contains synovial tissue biopsy specimens from RA patients (n = 10) and healthy controls (n = 10). The results similarly showed that AGTR1 expression in RA synovial tissue was significantly lower than that of healthy controls (right panel of **Figure 1A**), which was consistent with the GSE21959 results. Given that FLS are the predominant cell type in the synovial lining and play a central role in RA pathogenesis, we further examined AGTR1 expression in *in vitro*-cultured FLS. qRT-PCR and WB results (**Figure 1B**, **1C**) confirmed that both the mRNA and protein levels of AGTR1 in RA-FLS were significantly lower than those in normal FLS. Taken together, these findings indicated that AGTR1 was downregulated in RA, and this downregulation was closely associated with FLS.

AGTR1 modulates caspase-1, NLRP3, ASC, and GSDMD expression

In RA, FLS exhibit abnormal activation, hyperproliferation, invasiveness, and a tendency toward tumor-like transformation. Pro-inflammatory cytokines and MMPs secreted by these cells exacerbate inflammatory responses and joint cartilage destruction [9, 14, 18]. Compared to OA patients undergoing knee replacement surgery, synovial tissues from RA patients show higher GSDME-N expression, and GSDME-N expression in peripheral blood mononuclear cells of RA patients is significantly higher than in controls. Therefore, we hypothesized that the intrinsically high inflammatory state of RA-FLS accounts for the elevated levels of inflammation-related proteins. WB results indicated higher levels of key pyroptosis pro-

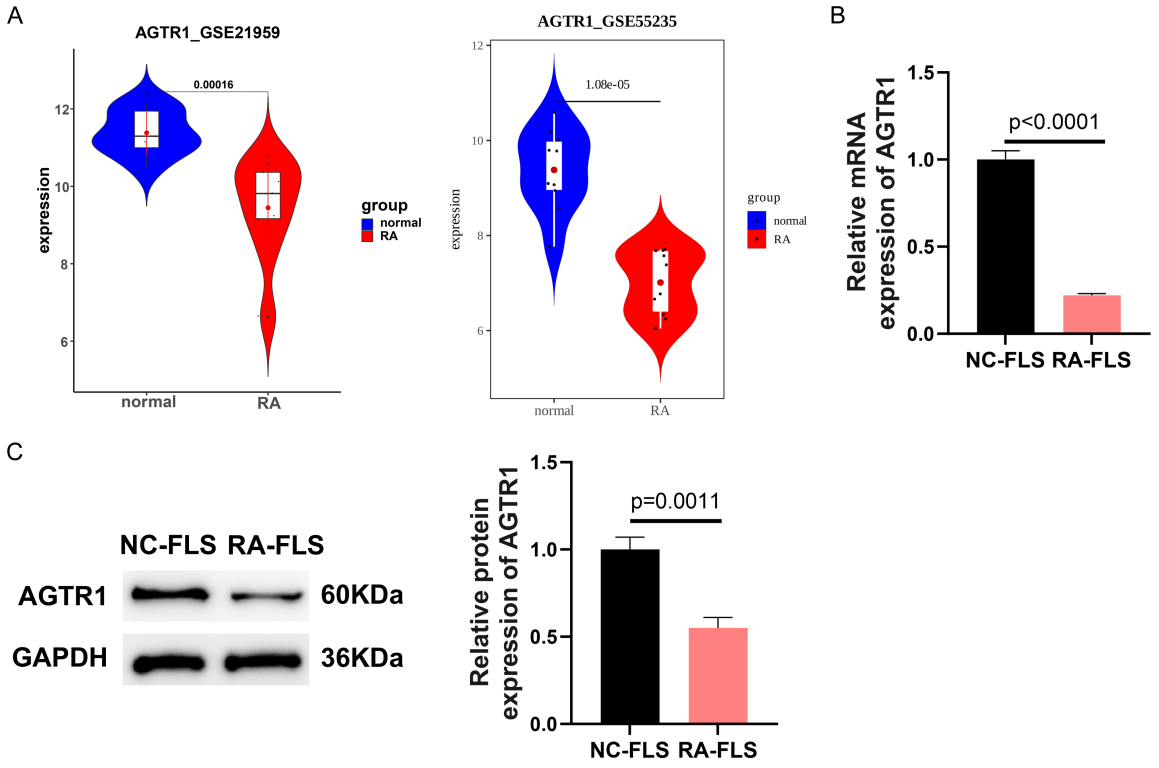

Figure 1. Downregulation of AGTR1 in RA. A. Bioinformatic analysis of AGTR1 expression in RA. Left panel: comparison of AGTR1 expression in the GSE21959 dataset between rheumatoid arthritis synovial fibroblasts (RA-SF, n = 9) and healthy synovial fibroblasts (HSF, n = 9). Right panel: comparison of AGTR1 expression in the GSE55235 dataset between RA synovial tissue (n = 10) and healthy control synovial tissue (n = 10). Blue, healthy control group; red, RA group. B. qRT-PCR analysis of AGTR1 mRNA levels in NC-FLS and RA-FLS. C. WB analysis of AGTR1 protein expression in NC-FLS and RA-FLS.

teins ASC and NLRP3 in RA-FLS cells than in NC-FLS cells (Supplementary Figure 1A, 1B). Caspase-1 is activated by ASC, and GSDMD-N directly mediates plasma membrane damage. Therefore, we quantified caspase-1, GSDMD-full, and the activated forms of cleaved caspase-1 and GSDMD-N levels in cells, which were substantially higher in RA-FLS cells than in NC-FLS cells (Supplementary Figure 1C-F). The findings supported the inherent inflammatory characteristics of RA-FLS cells.

Given the crucial roles of FLS pyroptosis in RA pathogenesis, we hypothesized that downregulated AGTR1 in RA-FLS might regulate pyroptosis. We established AGTR1-overexpressing RA-FLS by transfecting with oe-AGTR1. As shown in **Figure 2A-C**, qRT-PCR and WB confirmed successful AGTR1 overexpression. Transfected RA-FLS cells were stained (oe-NC and oe-AGTR1), and flow cytometry analysis showed that AGTR1-positive cells were significantly increased in the oe-AGTR1 group compared to the oe-NC (**Figure 2D**).

To examine AGTR1's effect on pyroptosis, cells were treated with pyroptosis inducer nigericin (10 nM) for 24 h. Nigericin treatment increased expression of key pyroptosis-related proteins ASC and NLRP3 by approximately 2-fold compared to controls. AGTR1 overexpression significantly attenuated this nigericin-induced upregulation (**Figure 2E**, **2F**). We examined caspase-1, GSDMD-full, activated cleaved caspase-1, and GSDMD-N levels in cells. While nigericin treatment did not alter total caspase-1 or GSDMD-full levels, it markedly increased activated cleaved caspase-1 and GSDMD-N (**Figure 2G-J**). AGTR1 overexpression (oe-AGTR1+Nigericin group) reduced nigericin-induced accumulation of these activated forms. AGTR1 overexpression suppressed nigericin-induced expression of pyroptosis-related proteins in RA-FLS.

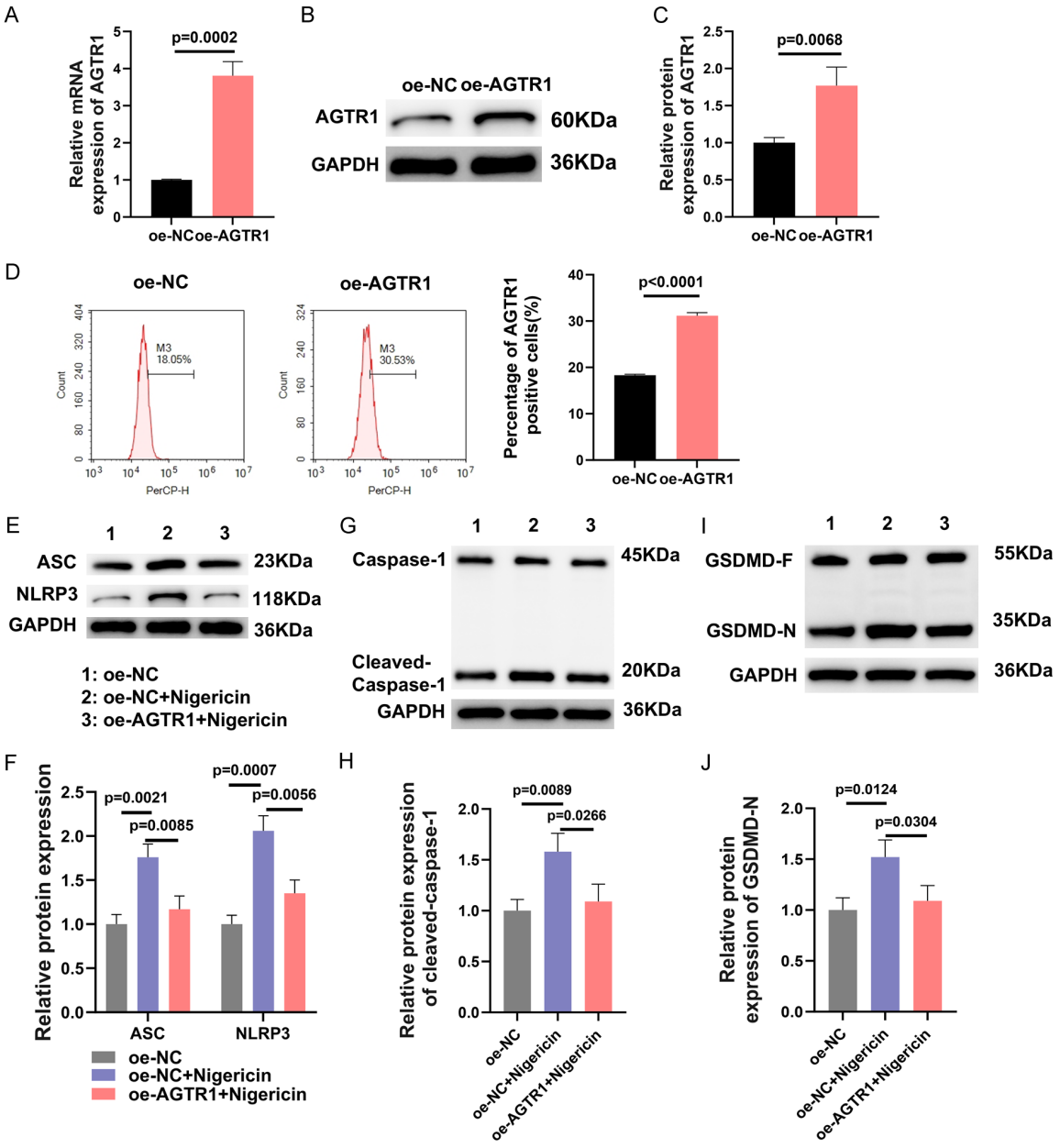

Figure 2. AGTR1 regulates expression of ASC, NLRP3, caspase-1, and GSDMD. A. qRT-PCR analysis of AGTR1 mRNA levels in FLS cells post-transfection of oe-AGTR1. B, C. WB analysis of AGTR1 protein expression in FLS post-transfection of oe-AGTR1. D. Expression detection of AGTR1 by flow cytometry. E, F. WB analysis of ASC and NLRP3 expression in cells treated with oe-NC, oe-NC+Nigericin, or oe-AGTR1+Nigericin. G-J. WB analysis of caspase-1, GSDMD-full, cleaved caspase-1, and GSDMD-N expression under different treatments in FLS.

AGTR1 modulates pyroptosis and inflammatory cytokine secretion

Having established AGTR1's inhibitory effect on pyroptosis-related proteins, we further examined its effect on FLS pyroptosis. Nigericin-treated cells were analyzed by TUNEL staining to assess apoptosis levels. Immunofluorescence (**Figure 3A**, **3B**) revealed significantly increased green fluorescence intensity in nigericin-treated cells compared with oe-NC controls, indicating DNA damage. oe-AGTR1+Nigericin group exhibited weaker green fluorescence signals than oe-NC+Nigericin cells, suggesting AGTR1 overexpression attenuated apoptosis to some extent. Flow cytometry analysis of cas-

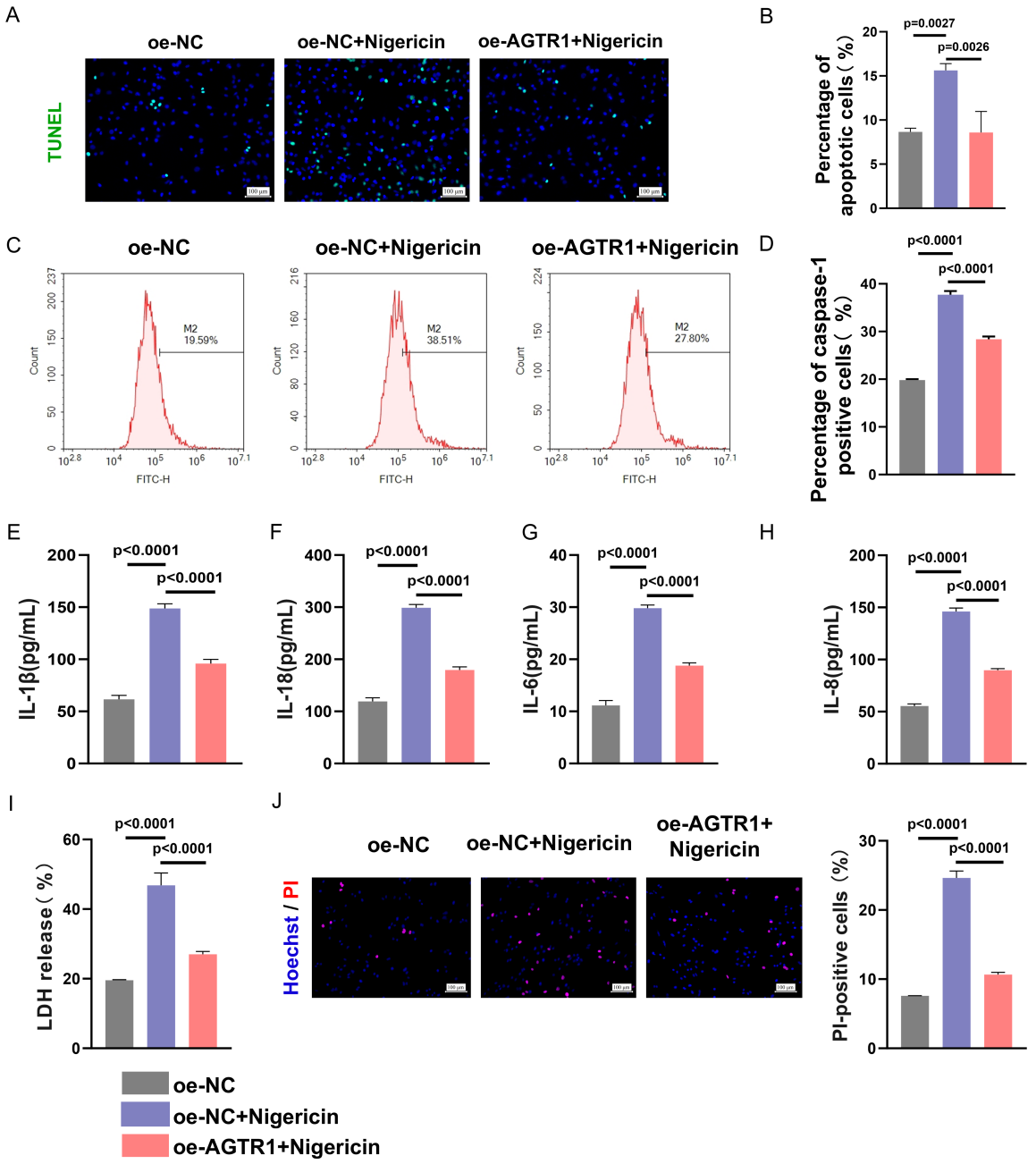

Figure 3. AGTR1 regulates pyroptosis and inflammatory cytokine secretion. A, B. TUNEL staining of FLS treated with oe-NC, oe-NC+Nigericin, or oe-AGTR1+Nigericin. C, D. Flow cytometry analysis of caspase-1-positive cells. E-H. ELISA measurement of IL-1β, IL-18, IL-6, and IL-8 levels in culture supernatants. I. LDH release assay of FLS with different treatments. J. Representative images of dual immunofluorescence staining for PI (red) and Hoechst 33342 (blue).

pase-1-positive cells (**Figure 3C**, **3D**) demonstrated that AGTR1 overexpression reduced caspase-1-positive cells from 36.82% to 27.60% under nigericin treatment, confirming that AGTR1 overexpression attenuated nigericin-induced FLS pyroptosis.

During RA progression, inflammatory cytokines (IL-1β, IL-18, IL-6, IL-8) were markedly elevated, playing pivotal roles in driving inflammation, joint destruction, and immune dysregulation. ELISA (**Figure 3E-H**) showed nigericin treatment nearly doubled cytokine secretion compared to

untreated controls, suggesting that induction of pyroptosis in FLS significantly enhanced the release of pro-inflammatory cytokines. AGTR1 overexpression significantly reduced nigericin-induced cytokine release. Consistent results were observed in LDH release assays (**Figure 3I**), where AGTR1 overexpression attenuated nigericin-induced LDH secretion. PI staining assays further demonstrated that nigericin treatment markedly increased the number of PI-positive cells, whereas AGTR1 overexpression effectively restored the proportion of PI-positive cells to levels comparable to those in the control group (**Figure 3J**). AGTR1 overexpression suppressed FLS pyroptosis and inflammatory cytokine secretion. To further confirm the necessary role of endogenous AGTR1 in RA-FLS pyroptosis, we generated AGTR1-knockdown cell lines. qRT-PCR and WB results showed that both the mRNA and protein levels of AGTR1 in the sh-AGTR1 group were significantly lower than those of the sh-NC group (Supplementary Figure 1G, 1H). After AGTR1 knockdown, the proportion of Caspase-1-positive cells was markedly increased (Supplementary Figure 1I). Also, the expression levels of the pyroptosis-related proteins ASC, NLRP3, GSDMD-F, and GSDMD-N were all significantly upregulated (Supplementary Figure 1J). In addition, ELISA results showed that the secretion levels of the pro-inflammatory cytokines IL-1β, IL-18, IL-6, and IL-8 in the cell culture supernatant of the sh-AGTR1 group were all significantly higher than those of the sh-NC group (Supplementary Figure 1K). The LDH release assay demonstrated that AGTR1 knockdown significantly increased LDH release into the cell culture supernatant (Supplementary Figure 1L), indicating aggravated disruption of plasma membrane integrity. Furthermore, PI/Hoechst double-staining revealed that AGTR1 knockdown significantly increased the proportion of PI-positive cells (Supplementary Figure 1M). Collectively, these results indicated that knockdown of AGTR1 exacerbated RA-FLS pyroptosis and promoted inflammatory cytokine release, confirming the indispensable role of endogenous AGTR1 in suppressing pyroptosis.

AGTR1 suppresses pyroptosis and inflammation through the TGF-β pathway

To elucidate the molecular mechanism underlying AGTR1's effects, we investigated TGF-β based on previous reports of AGTR1-TGF-β crosstalk in cancer [17]. As SMAD2/3 phosphorylation status reflects TGF-β pathway activation [19], we examined expression of TGF-β, P-SMAD, and total SMAD proteins in AGTR1 overexpressing RA-FLS cells by WB. AGTR1 overexpression significantly increased TGF-β, P-SMAD, and total SMAD protein levels (**Figure 4A**, **4B**), along with elevated P-SMAD/SMAD ratios (**Figure 4C**), indicating enhanced TGF-β pathway activation. To verify the regulatory function of the TGF-β pathway in FLS pyroptosis, we treated cells with the TGF-β receptor I inhibitor SB505124 or the TGF-β neutralizing antibody 1D11, and subsequently monitored alterations in multiple pyroptosis-associated biomarkers. As shown in **Figure 4D-F** and Supplementary Figure 2A-C, overexpressing AGTR1 in cells significantly downregulated pyroptosis-related proteins GSDMD-N, ASC, NLRP3, cleaved caspase-1, while increasing TGF-β protein levels. SB505124 or 1D11 treatment alone increased GSDMD-N, ASC, NLRP3, and cleaved caspase-1. However, administration of SB505124 or 1D11 in AGTR1-overexpressing cells restored the expression levels of these proteins, indicating that inhibition or blockage of the TGF-β pathway partially abrogates the anti-pyroptotic effect mediated by AGTR1. Further detection of cell apoptosis levels by TUNEL staining (**Figure 4G**, **4H**) revealed that overexpressing AGTR1 inhibited cell pyroptosis. SB505124 treatment promoted pyroptosis, and the addition of SB505124 on top of AGTR1 weakened the inhibitory effect of AGTR1 on cell apoptosis. Using caspase-1 to detect pyroptosis levels (**Figure 4I**, **4J**), we found that overexpressing AGTR1 inhibited pyroptosis in FLS cells. Furthermore, we examined inflammatory cytokine secretion and LDH release in cell supernatants using detection kits, and the results were consistent with the above findings. AGTR1 overexpression significantly suppressed the secretion of the four detected inflammatory cytokines and reduced LDH release. Treatment with SB505124 or 1D11 alone promoted inflammatory cytokine secretion and LDH release. Importantly, combined treatment with SB505124 or 1D11 partially reversed the inhibitory effects of AGTR1 overexpression and restored inflammatory cytokine production and LDH release (**Figure 4K-O** and Supplementary Figure 2D, 2E). PI staining showed that AGTR1 overexpression markedly reduced the number

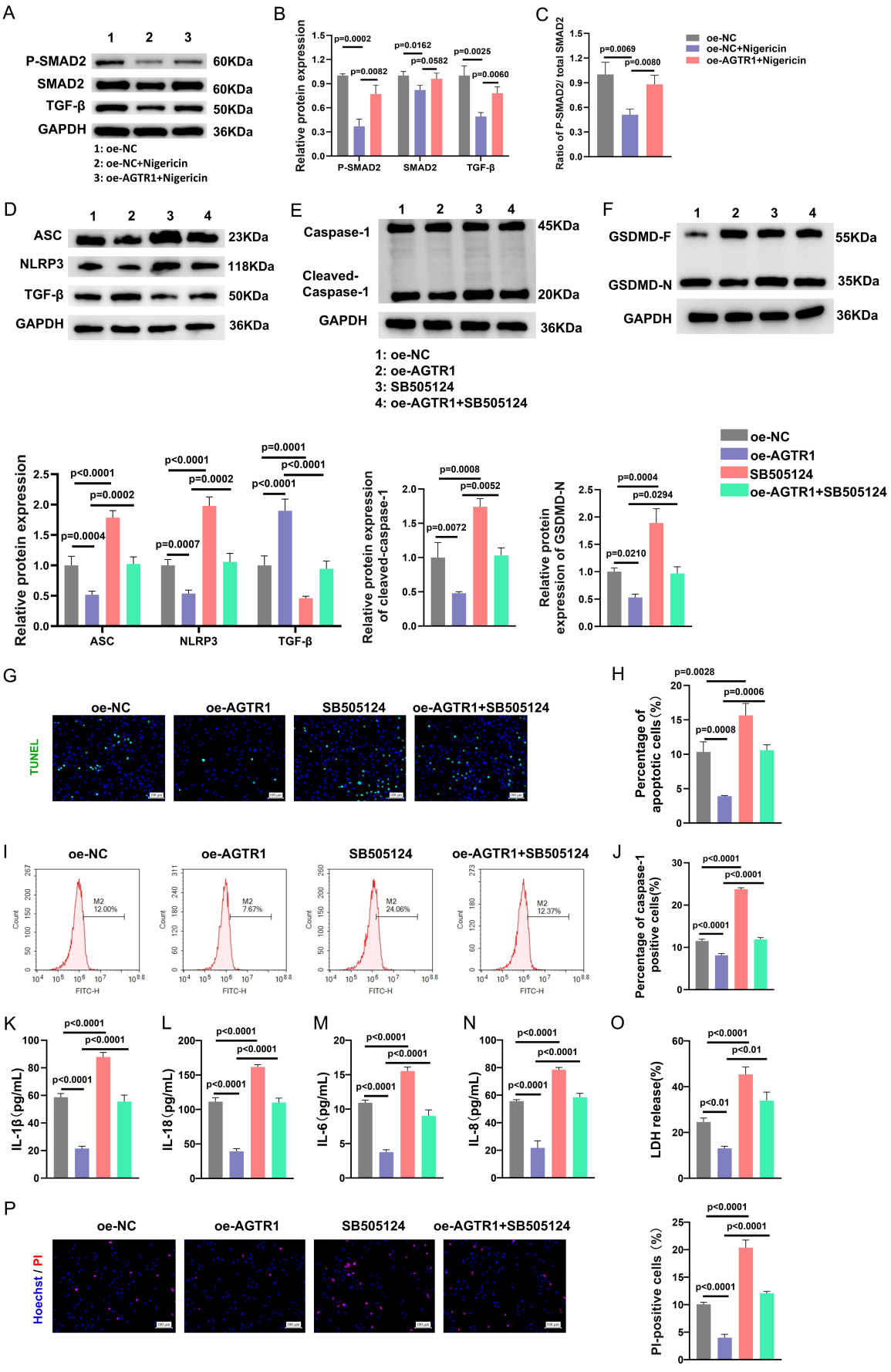
A
1 2 3
P-SMAD2 60KDa
SMAD2 60KDa
TGF-β 50KDa
GAPDH 36KDa
1: oe-NC
2: oe-NC+Nigericin
3: oe-AGTR1+Nigericin
B
Relative protein expression
P-SMAD2
SMAD2
TGF-β
C
Ratio of P-SMAD2/ total SMAD2
oe-NC
oe-NC+Nigericin
oe-AGTR1+Nigericin
D
ASC 23KDa
NLRP3 118KDa
TGF-β 50KDa
GAPDH 36KDa
E
Caspase-1 45KDa
Cleaved-Caspase-1 20KDa
GAPDH 36KDa
F
GSDMD-F 55KDa
GSDMD-N 35KDa
GAPDH 36KDa
1: oe-NC
2: oe-AGTR1
3: SB505124
4: oe-AGTR1+SB505124
oe-NC
oe-AGTR1
SB505124
oe-AGTR1+SB505124
Relative protein expression
ASC
NLRP3
TGF-β
Relative protein expression of cleaved-caspase-1
Relative protein expression of GSDMD-N
G
TUNEL
oe-NC
oe-AGTR1
SB505124
oe-AGTR1+SB505124
H
Percentage of apoptotic cells (%)
I
M2 12.00%
M2 7.67%
M2 24.06%
M2 12.37%
FITC-H
J
Percentage of caspase-1 positive cells(%)
K
IL-1β (pg/mL)
L
IL-18 (pg/mL)
M
IL-6 (pg/mL)
N
IL-8 (pg/mL)
O
LDH release(%)
P
Hoechst / PI
PI-positive cells (%)

Figure 4. AGTR1 inhibits FLS pyroptosis and inflammatory cytokine secretion through the TGF-β pathway. A, B. WB detection of P-SMAD2, SMAD2, and TGF-β expression in FLS cells treated with oe-NC, oe-NC+Nigericin, and oe-AGTR1+Nigericin. C. The ratio of P-SMAD2 to total SMAD2 in FLS cells. D-F. WB detection of ASC, NLRP3, cleaved caspase-1, and GSDMD-N protein expression levels in RA-FLS cells under Nigericin induction after treatment with oe-NC, oe-AGTR1, and oe-AGTR1+SB505124 (TGF-β receptor I inhibitor). G, H. TUNEL staining to assess apoptosis in FLS cells after different treatments. I, J. Flow cytometry detection of caspase-1-positive FLS cells after different treatments. K-N. ELISA measurement of inflammatory cytokines IL-1β, IL-18, IL-6, and IL-8 levels in the supernatant of FLS cells after different treatments. O. LDH release assay of FLS with different treatments. P. Representative images of dual fluorescence staining with PI (red) and Hoechst 33342 (blue).

of PI-positive cells compared to the control group, whereas additional SB505124 treatment significantly rescued this phenotype (**Figure 4P**). We used ELISA to detect inflammatory cytokine levels in cell supernatants and found that, consistent with the above results, overexpressing AGTR1 inhibited the secretion of the four inflammatory cytokines. SB505124 or 1D11 treatment alone promoted cytokine secretion, and the addition of SB505124 or 1D11 could partially increase cytokine secretion (**Figure 4K-N**). Furthermore, to further verify whether the regulatory effects of AGTR1 and the AGTR1-TGF-β signaling axis on pyroptosis observed in FLS cell lines possess clinical relevance, we conducted parallel experiments involving SB505124 treatment in primary FLS derived from patients with RA. Consistent with the above experimental results, SB505124 treatment efficiently blocked AGTR1-mediated activation of the TGF-β pathway and reversed the AGTR1-induced downregulation of pyroptosis-related proteins (GSDMD-N, ASC, NLRP3 and cleaved caspase-1) (Supplementary Figure 3A-F). ELISA and LDH release assays yielded concordant results: AGTR1 overexpression suppressed inflammatory cytokine secretion and LDH release, and such inhibitory effects could be partially reversed by SB505124 (Supplementary Figure 3G, 3H). Taken together, these data indicate that AGTR1 suppresses pyroptosis in FLS by activating the TGF-β pathway.

These results demonstrated that suppressive roles of AGTR1 on RA-FLS pyroptosis and inflammatory cytokine secretion were mediated through the TGF-β pathway. To ensure completeness of the setup, we added exogenous TGF-β1 (10 ng/mL) to function as a TGF-β1 agonist. We hypothesize that AGTR1 may suppress RA-FLS pyroptosis through activation of the TGF-β pathway. We thus included oe-NC, TGF-β1, oe-AGTR1, and oe-AGTR1 + TGF-β1 in Supplementary Figure 4. As presented in Supplementary Figure 4A-C, either AGTR1 overexpression or TGF-β1 treatment alone significantly lowered expression of pyroptosis-related proteins GSDMD-N, and cleaved caspase-1, ASC, NLRP3, while increasing TGF-β protein levels. When TGF-β1 was added to AGTR1-overexpressing cells, the relevant protein levels were further decreased or increased. TUNEL staining (Supplementary Figure 4D) indicated that either AGTR1 overexpression or TGF-β1 treatment alone attenuated cell pyroptosis, while the combination of TGF-β1 and AGTR1-overexpressing cells greatly suppressed cell death.

Discussion

Fibroblast-like synoviocytes (FLS) are critical in the pathogenesis of synovitis and joint destruction in RA [4, 20]. Therefore, this study focused on identifying regulators of FLS pyroptosis. AGTR1 was downregulated in RA synovial tissues and RA-FLS, while its overexpression suppressed nigericin-induced pyroptosis and inflammatory cytokine secretion in RA-FLS. The inhibitory effect was partially reversed by TGF-β receptor inhibition, revealing a novel regulatory mechanism of pyroptosis in FLS and identifying AGTR1 as a likely target for RA.

Cell death represents a fundamental process in cellular biology. While RA-FLS exhibit resistance to apoptosis - a non-inflammatory programmed cell death - they demonstrate excessive proliferation and aberrant behaviors, including increased inflammatory factor secretion and enhanced migratory and invasive capacities. Therefore, inducing apoptosis in RA-FLS may offer therapeutic benefits for RA treatment [21]. In contrast to apoptosis, pyroptosis is featured by a pro-inflammatory nature. Gasdermin proteins (GSDM) induce plasma membrane pores, causing osmotic lysis and release of inflammatory cytokines and damage-associated molecular patterns, thereby exacerbating inflammation [22, 23]. FLS hyper-

proliferation and pyroptosis, mediated by abnormal NLRP3 inflammasome activation, contribute significantly to joint destruction and inflammation in RA [24]. The positive correlation between NLRP3 and elevated inflammatory cytokines in RA patient sera and synovial fluid further supports this mechanism [25, 26]. In the CIA animal model, an upregulated NLRP3 inflammasome was observed in synovial FLS, along with increased MMP-1 in the supernatant. Elevated NLRP3 promotes secretion and maturation of IL-18/IL-1β through caspase-1 cleavage [27, 28]. These findings demonstrate that inflammasome-mediated pyroptosis is tightly associated with RA-FLS pathogenesis and exacerbates RA-related inflammatory responses. Our results extend this understanding by revealing significantly reduced AGTR1 expression in RA-FLS. Overexpression of AGTR1 markedly decreased levels of GSDMD-N, NLRP3, cleaved caspase-1, and ASC, thereby suppressing FLS pyroptosis and reducing inflammatory cytokine secretion. This finding confirms the critical role of pyroptosis in RA-FLS pathogenesis and suggests a strategy for mitigating FLS pyroptosis.

AGTR1 is a pivotal protein in blood pressure regulation that binds angiotensin II to induce vasoconstriction, sodium/water retention, and indirectly modulates inflammation, thrombosis, and fibrosis [29]. As a key component of the renin-angiotensin system (RAS), AGTR1 is critical in cardiovascular pathogenesis [30, 31]. AGTR1 may contribute to joint inflammatory disorders by modulating inflammatory factors and synovial fibroblast behavior. Angiotensin II/AGTR1 activation drives pathological changes in experimental OA mice, including subchondral bone sclerosis, synovitis, synovial damage, and articular cartilage degradation [32], highlighting AGTR1's pathogenic role in OA. TGF-β1 protects chondrocytes by repressing pyroptosis by Smad2/3 activation and NF-κB inhibition [12]. Although the study did not directly address AGTR1, the potential crosstalk between TGF-β and Ang II/AGTR1 signaling in inflammatory diseases [33, 34] implies the unexplored role of AGTR1 in RA.

We identified AGTR1's potential involvement in RA through bioinformatic analysis of synovial mRNA datasets and experimental validation in RA-FLS, revealing significant AGTR1 downregulation in RA. Functional assays demonstrated that AGTR1 overexpression suppressed nigericin-induced pyroptosis and cytokine secretion in FLS, while TGF-β receptor inhibition abolished this protective effect, indicating TGF-β-dependent regulation. Our findings not only establish AGTR1's impact on RA progression but also elucidate its mechanistic basis. However, we focused exclusively on AGTR1's canonical pyroptosis regulation. Whether non-canonical pathways contribute to effects of AGTR1 warrants further investigation. Furthermore, based on previous research [16, 35], as a core component of the RAS, the activation mode of TGF-β by AGTR1 has not been fully verified. Whether AGTR1 regulates inflammatory response and pyroptosis through non-SMAD-dependent pathways remains unexplored. Most importantly, the conclusions of the present study are currently supported only by evidence from cell lines and primary cells, and the *in vivo* functions of the AGTR1-TGF-β axis in RA require further validation using classic RA animal models such as CIA or humanized mice. In follow-up work, we aim to further investigate the role of non-canonical pathways in AGTR1-mediated regulation, clarify the precise mechanism by which AGTR1 activates TGF-β, and employ the CIA model to evaluate the impacts of AGTR1 overexpression or TGF-β pathway activation on synovial inflammation, articular cartilage destruction, and pyroptosis markers, to comprehensively validate the *in vivo* relevance of our findings.

Our study revealed that AGTR1 repressed FLS-RA pyroptosis and inflammatory cytokine secretion through TGF-β signaling. These findings suggest that targeted induction of AGTR1 expression or activation of TGF-β signaling may represent promising therapeutic strategies for mitigating FLS-mediated inflammation in RA.

Acknowledgements

This work was supported by Tianshan Talent Youth Science and Technology Top notch Talent Project in Xinjiang Uygur Autonomous Region (No. 2022TSYCJC0010); Karamay Key Scientific and Technological Innovation Talents Project; National Clinical Key Specialty Construction Project.

Disclosure of conflict of interest

None.

Address correspondence to: Zongbiao Bai, Department of Orthopaedics, Central Hospital of Karamay; Department of Orthopaedics, Karamay Hospital of People's Hospital of Xinjiang Uygur Autonomous Region, No. 120, Anding Road, Karamay 834000, Xinjiang, China. Tel: +86-18196010317; E-mail: dabiao924@126.com

References

[1] D'Orazio A, Cirillo AL, Greco G, Di Ruscio E, Latorre M, Pisani F, Alunno A and Puxeddu I. Pathogenesis of rheumatoid arthritis: one year in review 2024. Clin Exp Rheumatol 2024; 42: 1707-1713.

[2] Ding Q, Hu W, Wang R, Yang Q, Zhu M, Li M, Cai J, Rose P, Mao J and Zhu YZ. Signaling pathways in rheumatoid arthritis: implications for targeted therapy. Signal Transduct Target Ther 2023; 8: 68.

[3] DI Matteo A and Emery P. Rheumatoid arthritis: a review of the key clinical features and ongoing challenges of the disease. Panminerva Med 2024; 66: 427-442.

[4] Chen Y, Han T, Guo Z, Li X, Zhang X and Peng W. Editorial: immunomodulatory roles of fibroblast-like synoviocytes in rheumatoid arthritis. Front Immunol 2024; 15: 1415672.

[5] Han C, Li Y, Zhang Y, Wang Y, Cui D, Luo T, Zhang Y, Liu Q, Li H, Wang C, Xu D, Ma Y and Wei W. Targeted inhibition of GRK2 kinase domain by CP-25 to reverse fibroblast-like synoviocytes dysfunction and improve collagen-induced arthritis in rats. Acta Pharm Sin B 2021; 11: 1835-1852.

[6] Zhai Z, Yang F, Xu W, Han J, Luo G, Li Y, Zhuang J, Jie H, Li X, Shi X, Han X, Luo X, Song R, Chen Y, Liang J, Wu S, He Y and Sun E. Attenuation of rheumatoid arthritis through the inhibition of tumor necrosis factor-induced caspase 3/gasdermin e-mediated pyroptosis. Arthritis Rheumatol 2022; 74: 427-440.

[7] Liu Y, Pan R, Ouyang Y, Gu W, Xiao T, Yang H, Tang L, Wang H, Xiang B and Chen P. Pyroptosis in health and disease: mechanisms, regulation and clinical perspective. Signal Transduct Target Ther 2024; 9: 245.

[8] Xu J and Nunez G. The NLRP3 inflammasome: activation and regulation. Trends Biochem Sci 2023; 48: 331-344.

[9] Jiang P, Wei K, Chang C, Zhao J, Zhang R, Xu L, Jin Y, Xu L, Shi Y, Guo S, Schrodi SJ and He D. SFRP1 negatively modulates pyroptosis of fibroblast-like synoviocytes in rheumatoid arthritis: a review. Front Immunol 2022; 13: 903475.

[10] Yang P, Feng W, Li C, Kou Y, Li D, Liu S, Hasegawa T and Li M. LPS induces fibroblast-like synoviocytes RSC-364 cells to pyroptosis through NF-kappaB mediated dual signalling pathway. J Mol Histol 2021; 52: 661-669.

[11] Mao J, Tan M, Li J, Liu C, Hao J, Zheng J and Shen H. Neutrophil extracellular traps induce pyroptosis of rheumatoid arthritis fibroblast-like synoviocytes via the NF-kappaB/Caspase 3/GSDME pathway. Inflammation 2024; 47: 921-938.

[12] Wang Y, Jin Z, Jia S, Shen P, Yang Y and Huang Y. Mechanical stress protects against chondrocyte pyroptosis through TGF-beta1-mediated activation of Smad2/3 and inhibition of the NF-kappaB signaling pathway in an osteoarthritis model. Biomed Pharmacother 2023; 159: 114216.

[13] Deng Z, Fan T, Xiao C, Tian H, Zheng Y, Li C and He J. TGF-beta signaling in health, disease, and therapeutics. Signal Transduct Target Ther 2024; 9: 61.

[14] Mao X, Wu W, Nan Y, Sun W and Wang Y. SMAD2 inhibits pyroptosis of fibroblast-like synoviocytes and secretion of inflammatory factors via the TGF-beta pathway in rheumatoid arthritis. Arthritis Res Ther 2023; 25: 144.

[15] Geng Q, Wei Q, Wang S, Qi H, Zhu Q, Liu X, Shi X and Wen S. Physcion 8-O-beta-glucopyranoside extracted from Polygonum cuspidatum exhibits anti-proliferative and anti-inflammatory effects on MH7A rheumatoid arthritis-derived fibroblast-like synoviocytes through the TGF-beta/MAPK pathway. Int J Mol Med 2018; 42: 745-754.

[16] Yu Z, Kisner A, Bhatt A, Polter AM and Marvar PJ. Central amygdala angiotensin type 1 receptor (Agtr1) expressing neurons contribute to fear extinction. Neuropharmacology 2023; 229: 109460.

[17] Wang L, Li H, Zhang W, Ren M, Shao M and Wang J. AGTR1 blocker attenuates activation of Tenon's capsule fibroblasts after glaucoma filtration surgery via the NF-kappaB signaling pathway. Exp Cell Res 2021; 407: 112786.

[18] Nygaard G and Firestein GS. Restoring synovial homeostasis in rheumatoid arthritis by targeting fibroblast-like synoviocytes. Nat Rev Rheumatol 2020; 16: 316-333.

[19] Hu HH, Chen DQ, Wang YN, Feng YL, Cao G, Vaziri ND and Zhao YY. New insights into TGF-beta/Smad signaling in tissue fibrosis. Chem Biol Interact 2018; 292: 76-83.

[20] Jin L, Chen Q, Hu K, Fan D, Zhang H, Deng J, Qi W and Yu Q. The FTO-CMPK2 pathway in fibroblast-like synoviocytes modulates rheumatoid arthritis synovial inflammation and cartilage homeostasis via mtDNA regulation. Int J Biol Sci 2024; 20: 1617-1633.

[21] Meng Q, Wei K and Shan Y. E3 ubiquitin ligase gene BIRC3 modulates TNF-induced cell death pathways and promotes aberrant proliferation

in rheumatoid arthritis fibroblast-like synoviocytes. Front Immunol 2024; 15: 1433898.
[22] Broz P. Pyroptosis: molecular mechanisms and roles in disease. Cell Res 2025; 35: 334-344.
[23] Cai H, Zhang J, Xu H, Sun W, Wu W, Dong C, Zhou P, Xue C, Nan Y, Ni Y, Wu X, Gu Z, Chen M and Wang Y. ALOX5 drives the pyroptosis of CD4(+) T cells and tissue inflammation in rheumatoid arthritis. Sci Signal 2024; 17: eadh1178.
[24] Manca ML, Lattuada D, Valenti D, Marelli O, Corradini C, Fernandez-Busquets X, Zaru M, Maccioni AM, Fadda AM and Manconi M. Potential therapeutic effect of curcumin loaded hyalurosomes against inflammatory and oxidative processes involved in the pathogenesis of rheumatoid arthritis: the use of fibroblast-like synovial cells cultured in synovial fluid. Eur J Pharm Biopharm 2019; 136: 84-92.
[25] Burska A, Boissinot M and Ponchel F. Cytokines as biomarkers in rheumatoid arthritis. Mediators Inflamm 2014; 2014: 545493.
[26] Zhang Y, Zheng Y and Li H. NLRP3 inflammasome plays an important role in the pathogenesis of collagen-induced arthritis. Mediators Inflamm 2016; 2016: 9656270.
[27] Li XF, Shen WW, Sun YY, Li WX, Sun ZH, Liu YH, Zhang L, Huang C, Meng XM and Li J. MicroRNA-20a negatively regulates expression of NLRP3-inflammasome by targeting TXNIP in adjuvant-induced arthritis fibroblast-like synoviocytes. Joint Bone Spine 2016; 83: 695-700.
[28] Li Y, Zheng JY, Liu JQ, Yang J, Liu Y, Wang C, Ma XN, Liu BL, Xin GZ and Liu LF. Succinate/NLRP3 inflammasome induces synovial fibroblast activation: therapeutical effects of clematichinenoside AR on arthritis. Front Immunol 2016; 7: 532.
[29] Pan Y, Wang C, Zhou W, Shi Y, Meng X, Muhammad Y, Hammer RD, Jia B, Zheng H, Li DP, Liu Z, Hildebrandt G and Kang X. Inhibiting AGTR1 reduces AML burden and protects the heart from cardiotoxicity in mouse models. Sci Transl Med 2024; 16: eadl5931.
[30] Tran DC, Le LHG, Thai TT, Van Hoang S, Do MD and Truong BQ. Effect of AGTR1 A1166C genetic polymorphism on coronary artery lesions and mortality in patients with acute myocardial infarction. PLoS One 2024; 19: e0300273.
[31] Eivazi M, Hosseini K, Alipanahi S, Xia H, Restivo L, Patel A, Gozali M, Ebrahimi T, Scarborough A, Tarhriz V and Lazartigues E. Deep learning-driven proteomics analysis for gene annotation in the renin-angiotensin system. Eur J Pharmacol 2025; 1006: 178119.
[32] Chen Y, Zhang Y, Ge Y and Ren H. Integrated single-cell and bulk RNA sequencing analysis identified pyroptosis-related signature for diagnosis and prognosis in osteoarthritis. Sci Rep 2023; 13: 17757.
[33] Parichatikanond W, Duangrat R and Mangmool S. G(alphaq) protein-biased ligand of angiotensin II type 1 receptor mediates myofibroblast differentiation through TGF-beta1/ERK axis in human cardiac fibroblasts. Eur J Pharmacol 2023; 951: 175780.
[34] Ehanire T, Ren L, Bond J, Medina M, Li G, Bashirov L, Chen L, Kokosis G, Ibrahim M, Selim A, Blobe GC and Levinson H. Angiotensin II stimulates canonical TGF-beta signaling pathway through angiotensin type 1 receptor to induce granulation tissue contraction. J Mol Med (Berl) 2015; 93: 289-302.
[35] Lee JH and Massagué J. TGF-β in developmental and fibrogenic EMTs. Semin Cancer Biol 2022; 86: 136-145.

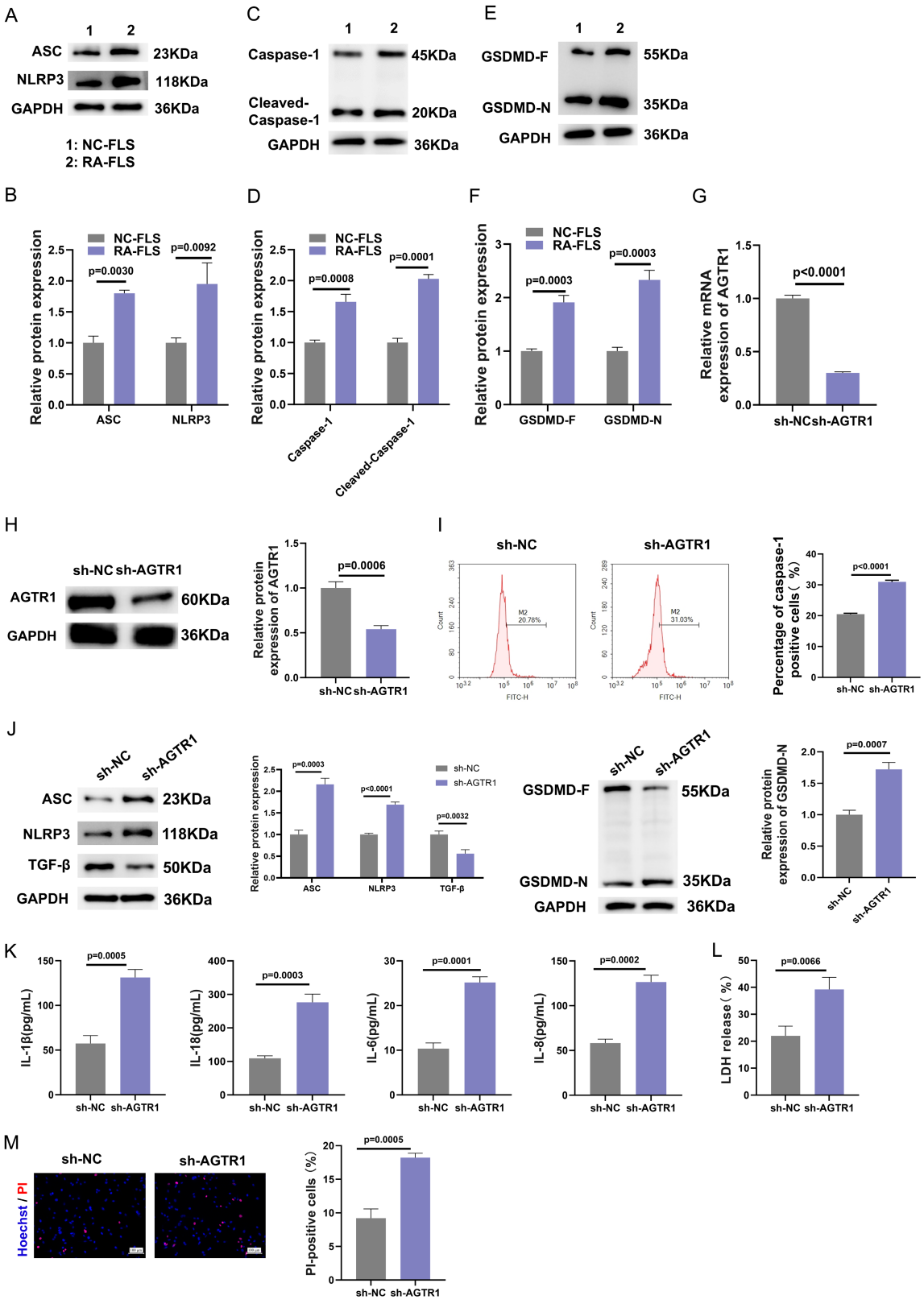

Supplementary Figure 1. A, B. WB analysis of ASC and NLRP3 protein expression in NC-FLS and RA-FLS cells. C, D. WB analysis of caspase-1 expression in NC-FLS and RA-FLS cells. E, F. WB analysis of GSDMD-full and GSDMD-N expression. G, H. WB and qRT-PCR analysis of AGTR1 expression in RA-FLS cells treated with sh-NC or sh-AGTR1. I.

Flow cytometric analysis of the proportion of Caspase-1-positive cells. J. WB analysis of ASC, NLRP3, and GSDMD-N protein expression levels in RA-FLS cells. K. ELISA measurement of the levels of the inflammatory cytokines IL-1β, IL-18, IL-6, and IL-8 in FLS cell culture supernatants. L. LDH release assay in FLS. M. Representative images of double-fluorescence staining with PI (red) and Hoechst 33342 (blue).

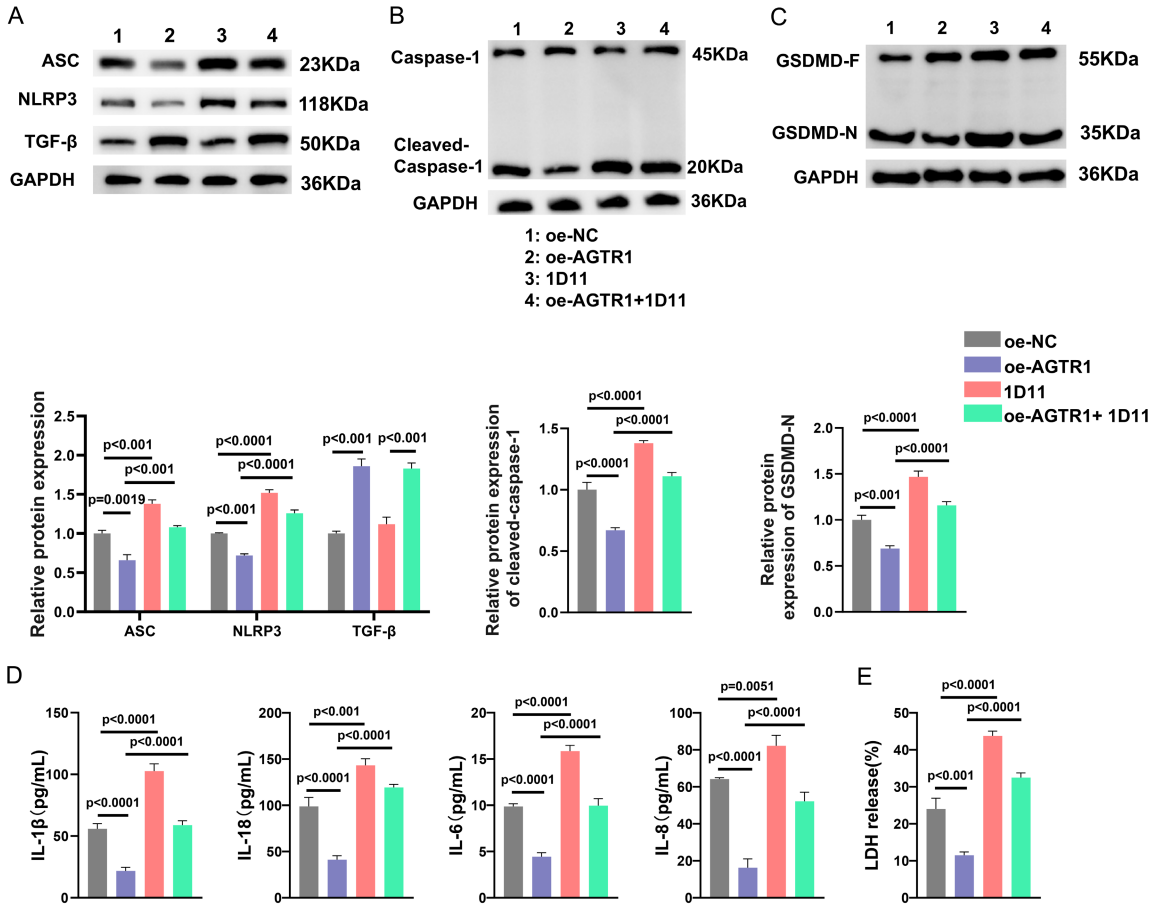

Supplementary Figure 2. A-C. WB detection of ASC, NLRP3, TGF-β, cleaved caspase-1, and GSDMD-N protein expression levels in RA-FLS cells under Nigericin induction after treatment with oe-NC, oe-AGTR1, and oe-AGTR1+1D11 (TGF-β neutralizing antibody). D. ELISA measurement of inflammatory cytokines IL-1β, IL-18, IL-6, and IL-8 levels in the supernatant of FLS cells after different treatments. E. LDH release assay of FLS with different treatments.

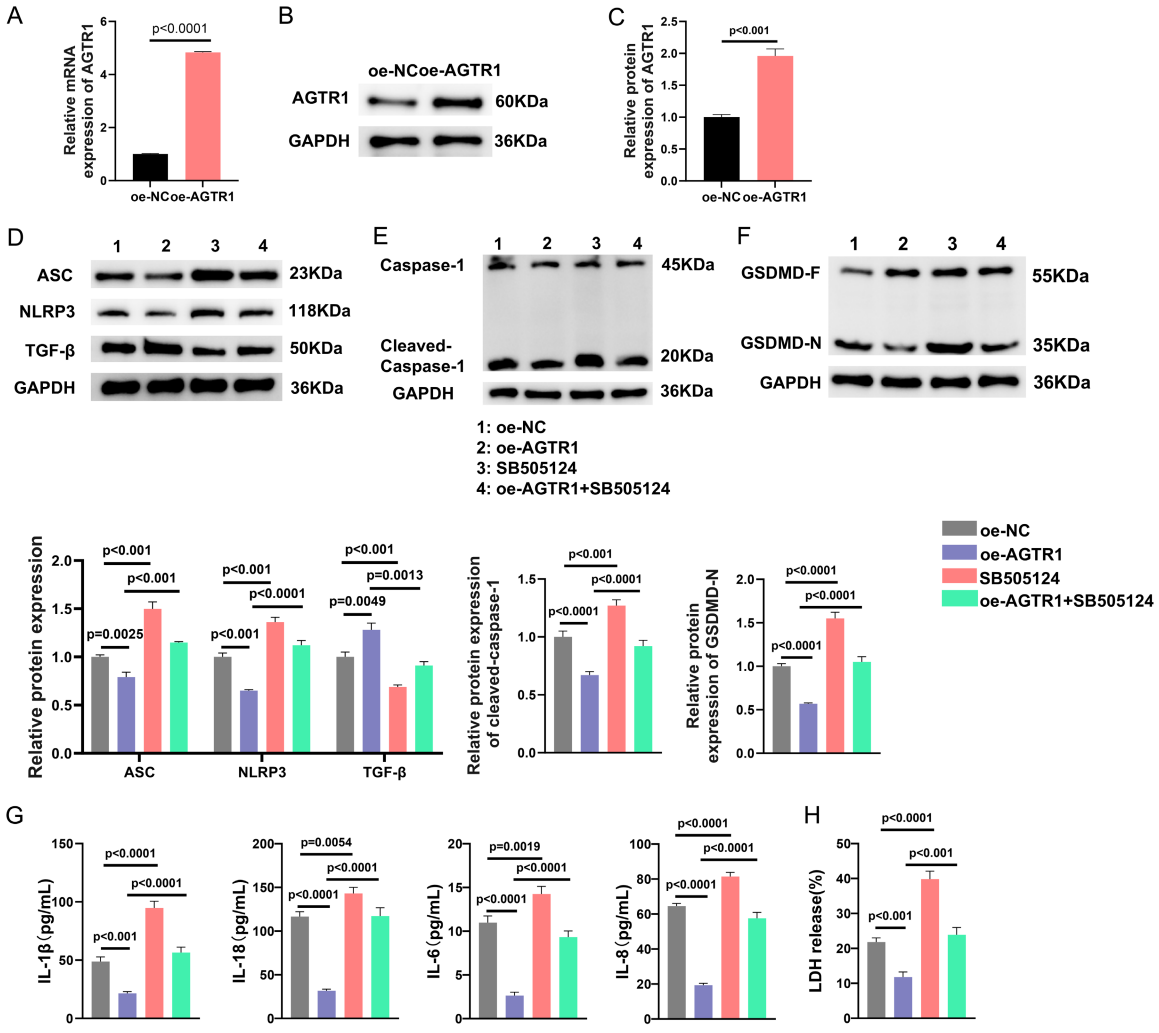

Supplementary Figure 3. A. qRT-PCR analysis of AGTR1 mRNA levels in primary FLS cells post-transfection of oe-AGTR1. B, C. WB analysis of AGTR1 protein expression in FLS post-transfection of oe-AGTR1. D-F. WB detection of ASC, NLRP3, cleaved caspase-1, and GSDMD-N protein expression levels primary FLS cells under Nigericin induction after treatment with oe-NC, oe-AGTR1, and oe-AGTR1+SB505124 (TGF-β receptor I inhibitor). G. ELISA measurement of inflammatory cytokines IL-1β, IL-18, IL-6, and IL-8 levels in the supernatant of FLS cells after different treatments. H. LDH release assay of primary FLS cells with different treatments.

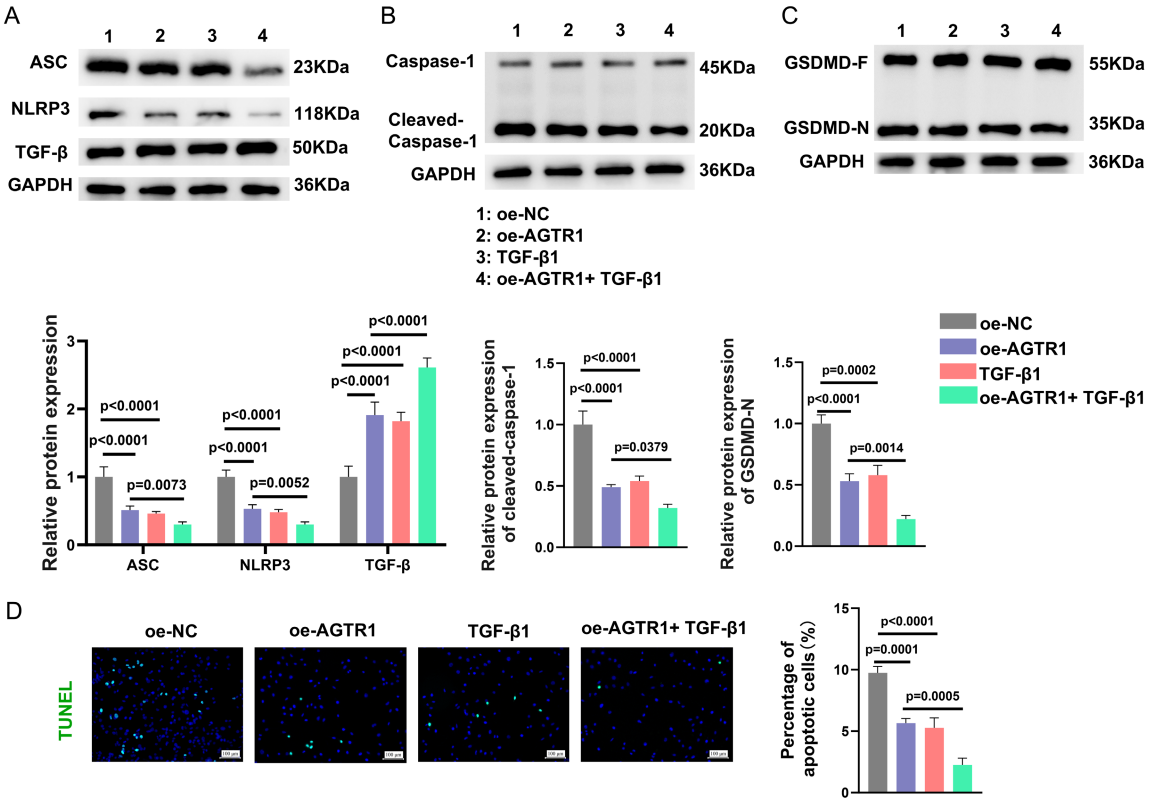

Supplementary Figure 4. A. WB detection of ASC, NLRP3, and TGF-β expression in FLS cells treated with oe-NC, oe-AGTR1, TGF-β1, oe-AGTR1+TGF-β1. B, C. WB detection of cleaved caspase-1, and GSDMD-N protein expression levels in RA-FLS cells treated with oe-NC, oe-AGTR1, TGF-β1, oe-AGTR1+TGF-β1. D. TUNEL staining to assess apoptosis in FLS cells after different treatments.